Distribution Category:
LMFBR--Safety (UC-79p)

ANL-80-31

ARGONNE NATIONAL LABORATORY
9700 South Cass Avenue
Argonne, Illinois 60439

ACCURATE NUMERICAL SOLUTIONS FOR ELASTIC-PLASTIC MODELS

by

H. L. Schreyer, R. F. Kulak,
and J. M. Kramer

Reactor Analysis and Safety Division

March 1980

TABLE OF CONTENTS

LIST OF FIGURES

TABLE

ACCURATE NUMERICAL SOLUTIONS FOR ELASTIC-PLASTIC MODELS

by

H. L. Schreyer, R. F. Kulak,
and J. M. Kramer

ABSTRACT

The accuracy of two integration algorithms is studied for the common engineering condition of a von Mises, isotropic hardening model under plane stress. Errors in stress predictions for given total strain increments are expressed with contour plots of two parameters; an angle in the pi plane and the difference between the exact and computed yield-surface radii. The two methods are the tangent-predictor/radial-return approach and the elastic-predictor/radial-corrector algorithm originally developed by Mendelson. The accuracy of a combined tangent-predictor/radial-corrector algorithm is also investigated. For single-step, constant-strain-rate increments, the elastic-predictor/radial-corrector method is generally the most accurate, although errors in angle can be significant. The use of a simple subincrementation formula with any one of the three approaches yields results that would be acceptable for most engineering problems.

I. INTRODUCTION

Computer codes that can handle elastic-plastic structural-response problems are being used routinely by analysts. Such codes are usually organized so that the constitutive equation is incorporated in a separate subroutine. For a given problem, this subroutine can be called thousands of times so that any error initiated by the constitutive-equation algorithm can be cumulative and lead to completely erroneous results. If the response is strictly elastic, the error is related to the word length of the machine. However, for elastic-plastic behavior the algorithm used can be a source of error that is larger by several orders of magnitude. In spite of the importance of understanding and controlling such an error, the subject has received little attention in the open literature. The object of this report is to show the numerical inaccuracy that is introduced by each of two common elastic-plastic algorithms and to indicate with examples how a simple formula for subincrementation can be used to limit the error in each case.

Krieg and Krieg[1] have performed a thorough analysis of the accuracy of integration of the constitutive equations for an isotropic elastic-perfectly plastic von Mises material. A selected range of directions of the strain-rate vector for various durations was studied and the solution for stress compared with an exact solution.[2] The secant, tangent-stiffness/radial-return, and simple-radial-return methods were considered. Each method was found to be most accurate for a region within the graph of strain-rate direction versus duration. The results of the study gave detailed guidelines for providing an error estimate and the suggestion that, for most engineering applications, the simplest algorithm was adequate.

If strain hardening is present, a corresponding error analysis is much more complicated. For the elastic-perfectly plastic case, the yield surface is fixed so that Krieg and Krieg[1] were able to use simply one parameter, an angle, as a measure of error. Also, they were able to use an exact solution that does not exist for the strain-hardening case. For strain-hardening models, the error in the size of the yield surface provides one more parameter that must be simultaneously investigated.

The next three sections summarize the basic theory for the elastic-predictor/radial-corrector and the tangent-predictor/radial-return schemes. Although it is not generally recognized, the former method is essentially that proposed by Mendelson.[3] In addition, the plane-stress versions of these theories are also given for two reasons. First, many engineering problems can be classified as plane stress, and second, certain aspects of the formulation are actually more complex for the two-dimensional case. The following two sections include a subincrementation scheme and contour plots of error for assumed load increments that include traversal from one side of the yield surface to the other. These results are limited to plane-stress conditions and the assumption of a constant-strain-rate vector for each step. Representative errors are given for cases when this latter assumption is violated.

Large computer codes that are used for the static or dynamic analysis of pressure vessels and piping require accurate and efficient constitutive-equation subroutines. Since the number of degrees of freedom is frequently very large, solutions are expensive and, consequently, load increments are also taken to be as large as possible. In the final section, recommendations based on this work are made for modifying elastic-plastic constitutive algorithms to limit the accumulation of error for problems that include complex loading sequences.

II. NOTATION

For convenience, components of all tensors are given in a rectangular Cartesian-coordinate system and the usual summation convention is used. For infinitesimal deformations, the deviatoric part of the strain rate can be

separated into the deviatoric part of the elastic strain rate and the plastic strain rate as follows:

$$\dot{e}_{ij} = \dot{e}^{e}_{ij} + \dot{e}^{p}_{ij}. \tag{1}$$

For isotropic materials, the deviatoric stress rate is given by

$$\dot{S}_{ij} = 2G\dot{e}^{e}_{ij}, \tag{2}$$

where G is the shear modulus, which is assumed to be constant. The plastic strain rate is determined from the associative potential flow law

$$\dot{e}^{p}_{ij} = \dot{\lambda}\frac{\partial\varphi}{\partial S_{ij}}, \tag{3}$$

where $\dot{\lambda}$ is a positive scalar function and φ is the yield function. For a step of finite duration, this equation is the source of the various approximations used in plasticity theory. The integration to obtain increments in components of the plastic-strain tensor is usually replaced by the finite sum

$$\Delta e^{p}_{ij} \simeq \sum_{n=1}^{N}\left(\bar{\Delta}\lambda\frac{\partial\varphi}{\partial S_{ij}}\right)_n, \tag{4}$$

in which $\bar{\Delta}\lambda$ represents the increment in λ over a subincrement in time $\bar{\Delta}t$ and the total time span is given by

$$\Delta t = N\bar{\Delta}t. \tag{5}$$

For an isotropic-hardening, von Mises model of a material, this yield function can be given in the form

$$\varphi(S_{ij}, \bar{\epsilon}^{p}) = S_{ij}S_{ij} - R^2(\bar{\epsilon}^{p}), \tag{6}$$

in which R, the radius of a hypersphere in deviatoric stress space, is related to a universal response function (such as the yield function, H, of a uniaxial stress specimen) by

$$R = \sqrt{\tfrac{2}{3}}H(\bar{\epsilon}^{p}). \tag{7}$$

The plastic-strain invariant, $\bar{\epsilon}^{p}$, is proportional to the path length in plastic-strain space

$$\bar{\epsilon}^{p} = \int_0^{t_1}\left(\tfrac{2}{3}e^{p}_{ij}e^{p}_{ij}\right)^{1/2}dt, \tag{8}$$

in which the parameter t increases monotonically from 0 to t_1 as the load is applied.

Suppose that, as a result of previous calculations, the deviatoric stress state S_{ij}^0 is known. For a given increment in total strain deviator, Δe_{ij}, obtained under the assumption of a constant strain rate, the object is to determine the final values of stress, elastic-strain, and plastic-strain deviators denoted by S_{ij}^F, e_{ij}^{eF}, and e_{ij}^{pF}, respectively. Since a purely elastic step is not of interest, the trial state, S_{ij}^T, found by the elastic relation

$$S_{ij}^T = S_{ij}^0 + 2G\Delta e_{ij}, \tag{9}$$

is assumed to fall outside the yield surface; i.e.,

$$\varphi\left(S_{ij}^T, \bar{\epsilon}_0^p\right) > 0, \tag{10}$$

in which $\bar{\epsilon}_0^p$ is the value of the plastic-strain invariant at the beginning of the step. The final values of the state variables must satisfy the yield (or consistency) condition

$$\varphi\left(S_{ij}^F, \bar{\epsilon}_F^p\right) = 0, \tag{11}$$

in addition to the other governing field equations.

For the frequently encountered plane-stress condition, the use of three-dimensional deviatoric stress-rate and strain-rate relations leads to an incompatibility between the final stresses and strains. In any algorithm, this inconsistency can be resolved by iteratively satisfying the constitutive equations, but the procedure is time-consuming. A more efficient approach is to use a formulation based on the stress components, σ_{ij}, and the strain components, ϵ_{ij}, rather than just the deviatoric parts.

III. ELASTIC-PREDICTOR/RADIAL-CORRECTOR METHOD

The procedure described in this section is essentially due to Mendelson,[3] who deserves considerable credit for introducing a very efficient scheme. The basic idea is that a trial state based on an elastic assumption is first obtained. Then the stress is corrected radially simultaneously with an adjustment in $\bar{\varepsilon}^p$, or yield-surface radius, until the consistency condition is satisfied. The theory assumes a particularly simple form in three dimensions, but for plane stress, the governing equations are slightly more complicated. Perhaps this is the reason the method has not been widely used.

If a one-step backward Euler integration procedure is used instead of Eq. 4, then, with the use of Eq. 6,

$$\Delta e_{ij}^p = 2\Delta\lambda S_{ij}^F. \tag{12}$$

The definition of the plastic-strain invariant from Eq. 8 and the requirement of Eq. 11 implies that

$$\Delta\bar{\varepsilon}^p = 2\sqrt{\tfrac{2}{3}}\Delta\lambda R_F, \tag{13}$$

where

$$R_F = R(\bar{\varepsilon}_F^p) = \sqrt{\tfrac{2}{3}}H(\bar{\varepsilon}_0^p + \Delta\bar{\varepsilon}^p). \tag{14}$$

The final and trial components of the elastic-strain deviator are related by

$$e_{ij}^{eF} = e_{ij}^{eT} - \Delta e_{ij}^p. \tag{15}$$

Then the use of Eqs. 15, 9, and 12 yields

$$S_{ij}^F = 2Ge_{ij}^{eF} = S_{ij}^T - 4G\Delta\lambda S_{ij}^F, \tag{16}$$

or

$$S_{ij}^F = S_{ij}^T/(1 + 4G\Delta\lambda). \tag{17}$$

The final stress state is proportional to the trial stress state; hence, the procedure is properly called a radial-correction method. However, the magnitude of the correction depends on $\Delta\lambda$, which must be determined.

The second invariant, $\bar{S}_T$, and effective stress, $\bar{\sigma}_T$, are defined by

$$\bar{S}_T = \left(S_{ij}^T S_{ij}^T\right)^{1/2} \tag{18}$$

and

$$\bar{\sigma}_T = \sqrt{\tfrac{3}{2}}\bar{S}_T. \tag{19}$$

Then, the result of taking the inner product of each side of Eq. 17 with itself is

$$R_F = \bar{S}_T/(1 + 4G\Delta\lambda), \tag{20}$$

in which Eq. 11 has been used. The substitution of Eqs. 7, 13, and 14 in Eq. 20 yields

$$\Delta\bar{\epsilon}^p = \frac{\bar{\sigma}_T - H(\bar{\epsilon}_0^p + \Delta\bar{\epsilon}^p)}{3G + H}. \tag{21}$$

Since $\bar{\sigma}_T$ is known from Eqs. 9, 18, and 19, and H is a specified function, this equation is easily solved numerically for $\Delta\bar{\epsilon}^p$. The final components for the stress deviator and strain deviator are obtained by back substitution in the appropriate equations.

For elastic-perfectly plastic material, R_F equals R_0, a fixed value, and the substitution of Eq. 20 in Eq. 17 yields

$$S_{ij}^F = \frac{R_0}{\bar{S}_T} S_{ij}^T, \tag{22}$$

which defines what is often called the radial-return method.[1]

For plane or uniaxial stress, components of the elastic-strain tensor, ϵ_{ij}^e, must be used and the convenience associated with the purely deviatoric formulation in three dimensions is lost. It can be easily shown that, for uniaxial stress, Eq. 21 reduces to the conventional one-dimensional relation

$$\Delta\bar{\epsilon}^p = \frac{\bar{\sigma}_T - H(\bar{\epsilon}_0^p + \Delta\bar{\epsilon}^p)}{E}. \tag{23}$$

For plane stress ($\sigma_{13} = \sigma_{23} = \sigma_{33} = 0$), the final and trial components of the elastic-strain tensor are related by

$$\left.\begin{aligned} \epsilon_{11}^{eF} &= \epsilon_{11}^{eT} - \Delta e_{11}^p, \\ \epsilon_{22}^{eF} &= \epsilon_{22}^{eT} - \Delta e_{22}^p, \end{aligned}\right\} \tag{24}$$

and

$$\left.\begin{aligned} \epsilon_{12}^{eF} &= \epsilon_{12}^{eT} - \Delta e_{12}^p, \end{aligned}\right\}$$

which correspond to Eq. 15. If these components are substituted in the elastic constitutive relations for plane stress, the result is

$$\left.\begin{aligned} \sigma_{11}^F &= \left(f\sigma_{11}^T + g\sigma_{22}^T\right)\Big/(f^2 - g^2), \\ \sigma_{22}^F &= \left(f\sigma_{22}^T + g\sigma_{11}^T\right)\Big/(f^2 - g^2), \end{aligned}\right\} \tag{25}$$

and

$$\sigma_{12}^F = \sigma_{12}^T \Big/ \left(1 + \frac{3}{2}\frac{G\Delta\bar{\epsilon}^P}{H_F}\right),$$

where

$$\left.\begin{aligned} f &= 1 + g\,\frac{2 - \nu}{1 - 2\nu}, \\ g &= \frac{1 - 2\nu}{1 - \nu}\,\frac{G\Delta\bar{\epsilon}^P}{H_F}, \end{aligned}\right\} \tag{26}$$

and ν denotes Poisson's ratio. The use of the expression for the effective stress in two dimensions yields

$$H_F \equiv H(\bar{\epsilon}_0^P + \Delta\bar{\epsilon}^P) = \left[\left(\sigma_{11}^F\right)^2 + \left(\sigma_{22}^F\right)^2 - \sigma_{11}^F\sigma_{22}^F + 3\left(\sigma_{12}^F\right)^2\right]^{1/2}, \tag{27}$$

which, together with Eq. 25, results in an equation that can be solved numerically for $\Delta\bar{\epsilon}^P$. Back substitution again yields the required values of the state functions.

IV. TANGENT-PREDICTOR/RADIAL-RETURN METHOD

This section briefly summarizes the tangent stiffness approach,[4,5] which has been developed and extensively used for some time. In this method, when the beginning-of-step stress state S_{ij}^0 lies within the yield surface, the step must be divided into two parts: elastic and elastoplastic. The elastic response brings the stress state in contact with the yield surface at the point S_{ij}^c, which is given by

$$S_{ij}^c = S_{ij}^0 + 2G\dot{e}_{ij}\Delta t_e, \tag{28}$$

where Δt_e is that part of the time step Δt which is purely elastic. For the plastic part of the step, the stress-deviator increment is related to the strain-rate deviator by

$$\Delta S_{ij} = 2G\dot{e}_{ij}^e\Delta t_p = 2G\left(\dot{e}_{ij} - \dot{e}_{ij}^p\right)\Delta t_p, \tag{29}$$

where the plastic-strain rate is determined from Eq. 3 and $\Delta t_p = \Delta t - \Delta t_e$. During plastic loading, the stress must lie on the yield surface. If the consistency condition of Eq. 6 is used in differential form, then

$$\frac{1}{2}\dot{\varphi} = S_{ij}\dot{S}_{ij} - R\dot{R} = 0. \tag{30}$$

The temporal derivative of the hardening function, which depends only on the accumulated plastic strain, is given by

$$\dot{R} = \frac{dR}{d\bar{\epsilon}_p}\dot{\bar{\epsilon}}_p. \tag{31}$$

With the plastic modulus defined by

$$E_p = \frac{dH}{d\bar{\epsilon}^p}, \tag{32}$$

the use of Eqs. 3, 6, and 8 yields the form

$$\dot{R} = \tfrac{4}{3}\dot{\lambda}RE_p. \tag{33}$$

Then Eqs. 1, 2, 3, 6, and 8 can be used to solve for

$$\dot{\lambda} = \frac{S_{ij}\dot{e}_{ij}}{2R^2\left(1 + \dfrac{E_p}{3G}\right)}. \tag{34}$$

The trial stress is calculated from Eqs. 9, 28, and 29. The result is

$$S_{ij}^T = S_{ij}^c + 2G\dot{e}_{k\ell}\left[\delta_{ik}\delta_{j\ell} - \frac{S_{k\ell}^c S_{ij}^c}{R^2\left(1 + \dfrac{E_p}{3G}\right)}\right]\Delta t_p, \tag{35}$$

in which δ_{ij} denote components of the identity tensor. In general, at the end of this calculation, since S_{ij}^T will not lie on the yield surface $R(\bar{\epsilon}_p^T)$, the stress is brought radially to the yield surface by

$$S_{ij}^F = rS_{ij}^T, \tag{36}$$

where S_{ij}^F satisfies

$$\varphi_F = S_{ij}^F S_{ij}^F - R^2(\bar{\epsilon}_p^T) = 0, \tag{37}$$

and the adjusting factor r is given by

$$r = \frac{R(\bar{\varepsilon}_p^T)}{\bar{S}^T} = \frac{H(\bar{\varepsilon}_p^T)}{\bar{\sigma}^T}. \tag{38}$$

As mentioned previously, it is more efficient to use stress-strain relations for plane-stress problems. For convenience, the three independent components of stress and strain are represented in a three-dimensional space. Then the stress-rate/strain-rate relation takes the form

$$\{\dot{\sigma}\} = [C]\{\dot{\epsilon}\}, \tag{39}$$

where

$$\{\dot{\sigma}\} = \{\dot{\sigma}_{11}, \dot{\sigma}_{22}, \dot{\sigma}_{12}\}^T \tag{40}$$

and

$$\{\dot{\epsilon}\} = \{\dot{\epsilon}_{11}, \dot{\epsilon}_{22}, 2\dot{\epsilon}_{12}\}^T, \tag{41}$$

with a superscript T denoting transpose. The material-property matrix is denoted by [C], which for elastic material behavior is given by

$$[C^e] = \frac{E}{1 - \nu^2}\begin{bmatrix} 1 & \nu & 0 \\ \nu & 1 & 0 \\ 0 & 0 & \frac{1 - \nu}{2} \end{bmatrix}, \tag{42}$$

and for elastoplastic behavior (see Ref. 6 for details) is

$$[C^p] = \frac{E}{Q}\begin{bmatrix} S_{22}^2 + 2P & -S_{11}S_{22} + 2\nu P & -\frac{S_{11} + \nu S_{22}}{1 + \nu} S_{12} \\ & S_{11}^2 + 2P & -\frac{S_{22} + \nu S_{11}}{1 + \nu} S_{12} \\ \text{Symmetric} & & \frac{T}{2(1 + \nu)} \end{bmatrix}, \tag{43}$$

$$\frac{2E_p}{9E}(1 - \nu)\bar{\sigma}^2$$

in which E and $\bar{\sigma}$ denote Young's modulus and the equivalent stress, respectively, and

$$P = \frac{2E_p}{9E}\bar{\sigma}^2 + \frac{\sigma_{12}^2}{1 + \nu}, \tag{44}$$

$$T = S_{11}^2 + 2\nu S_{11}S_{22} + S_{12}^2, \tag{45}$$

and

$$Q = T + 2(1 - \nu^2)P. \tag{46}$$

The plane-stress counterpart of Eq. 35 is given by

$$\{\sigma^T\} = \{\sigma^C\} + [C^P]\{\dot{\epsilon}\}\Delta t_p. \tag{47}$$

The trial stress is radially returned to the yield surface according to the relation

$$\{\sigma^F\} = r\{\sigma^T\}, \tag{48}$$

where r is computed from Eq. 38 and $\bar{\sigma}_T$ is given by

$$\bar{\sigma}_T = \left[\left(\sigma_{11}^T\right)^2 - \sigma_{11}^T\sigma_{22}^T + \left(\sigma_{22}^T\right)^2 + 3\left(\sigma_{12}^T\right)^2\right]^{1/2}. \tag{49}$$

V. SUBINCREMENTATION

Results obtained by using the method of subincrementation indicate that, for large strain increments, the final stress state can be substantially in error, even when the velocity strain is constant during the time increment. To reduce this error requires a subincrementing scheme. Several approaches are possible. For example, Bushnell[7] recommends that the number of subincrements be proportional to the equivalent-strain increment. In this section, a formula for computing the number of subincrements is developed on the basis that this number should depend on the plastic-strain-rate direction. Then the amount of subincrementation can be related to the desired level of accuracy to provide a computationally efficient algorithm.

To begin, assume that the stress state has been advanced to the yield surface, and consider this stress to be the contact stress S^c_{ij} in the following discussion. Note that the quantity $g_{ij} \equiv \partial f/\partial S_{ij}$ is a generalized vector normal to the yield surface. At the beginning of the step, the normal g^c_{ij} is known and the change in plastic-strain increment Δe^p_{ij} that occurs during the step must be determined. This increment is given by

$$\Delta e^p_{ij} = \int_{t_c}^{t_F} \dot{e}^p_{ij}\, dt = \int_{t_c}^{t_F} g_{ij}(t)\dot{\lambda}(t)dt, \tag{50}$$

in which the time of initial plastic deformation is denoted by t_c and the time at the end of the step by t_F. The rightmost integral above can be approximated as a sum as follows:

$$\Delta e^p_{ij} = \sum_{n=1}^{N} g^{(n)}_{ij}\dot{\lambda}(n)\Delta t(n). \tag{51}$$

When N tends to infinity, the sum equals the integral. When N is equal to 1 we have a single-step procedure. In single-step procedures, the assumption is usually made that during the time step the strain increment is small enough that the normal does not change significantly; thus the strain increment is given by

$$\Delta e^p_{ij} = g_{ij}\dot{\lambda}\Delta t, \tag{52}$$

in which $g_{ij} = g^c_{ij}$ for the tangent predictor and $g_{ij} = g^{tr}_{ij}$, the trial-state normal, for the elastic predictor. For either procedure, the end-of-step normal can be compared to the beginning-of-step normal to determine if the above assumption is valid. If the two normals are nearly equal, then the computed stress will also be quite accurate. On the other hand, if the normals differ significantly, the plastic-strain increment should be calculated by Eq. 51, where the number of subincrements, N, must be determined with an appropriate equation.

An estimate of the possible error for a given step is given by the angle between the beginning-of-step normal and the trial-state normal, that is,

$$\theta_T = \cos^{-1} \frac{S_{ij}^c S_{ij}^T}{\bar{S}^c \bar{S}^T}. \tag{53}$$

For plane stress, the trial-state stress and the trial-state deviatoric stress, S_{ij}^T, are obtained from the elastic constitutive relations for the elastic predictor and from Eq. 35 for the tangent predictor. However, if $\theta_T = 0$, the normal can still vary between the beginning and the end of the step, because of the simultaneous use of the plane-stress assumption; for the three-dimensional case, the unit normal would not change. However, the variation is probably small and subincrements would not be justified. When θ_T is not zero, a simple formula for the number of subincrements is

$$N = 1 + \frac{\theta_T}{k}, \tag{54}$$

in which θ_T is given in degrees and k is a positive number chosen on the basis of numerical experience. An example that uses this formula is given in the next section.

VI. ERROR ANALYSIS

The condition of plane stress was used to evaluate the accuracy of the two approaches, since this case introduces certain complicating features that are not present in a three-dimensional analysis. Also, it is probably the most important case for engineering applications. In addition, to limit the number of parameters, the material was assumed to be bilinear so that

$$H = H_0 + E_p \bar{\epsilon}^p, \tag{55}$$

in which H_0 and E_p are constants.

Although the assumption of plane stress was made, the results of the error analysis were presented in principal-deviatoric-stress space. The primary purpose for doing so was to permit easy comparison with the work of Krieg and Krieg,[1] which quite clearly forms the basis for this work. Following their approach, the initial deviatoric stress, S_{ij}^0, is taken to be on the yield surface with radius R_0. As shown on the pi plane in Fig. 1, this initial contact point has the coordinates $R_0(0, 1, -1)/\sqrt{2}$ and the associated unit vector defines the radial direction. The direction cosines of the unit tangential vector at this point, $(2, -1, 1)/\sqrt{6}$, are obtained by taking the cross product of the unit radial vector and the unit vector normal to the pi plane.

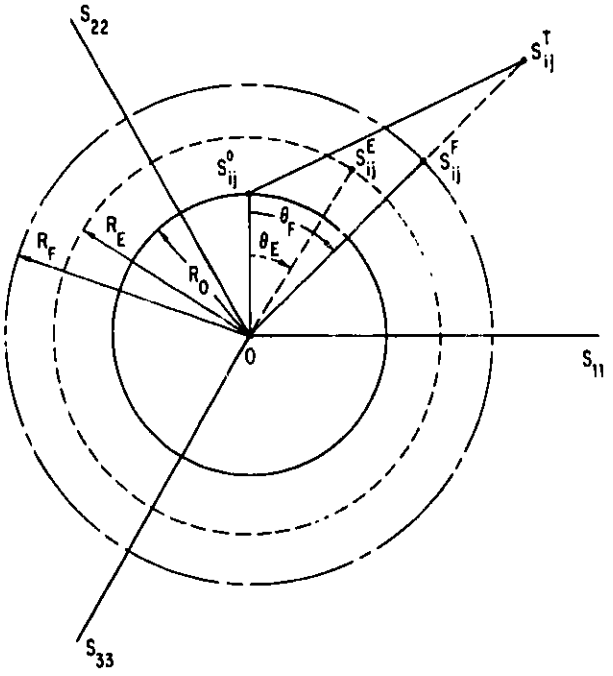

Fig. 1

Illustration in Pi Plane of Parameters Used for Error Analysis

Numerical calculations were made for various increments from the point S^0_{ij}. Each increment consisted of radial and tangential components

$$\left.\begin{aligned} \Delta S_r &= rR_0 \\ \text{and} \\ \Delta S_t &= tR_0 \end{aligned}\right\}, \tag{56}$$

in which r and t ranged from -5 to 5. One reason for choosing negative values was to show the lack of symmetry that the assumption of plane stress introduced as compared to the three-dimensional case.[1] Another reason was to assess accuracy when the yield surface is traversed. This aspect may require separate logic within an algorithm and can be the source of error.

With the restriction of plane stress, any principal stress state can be uniquely defined by two polar coordinates (R, θ) in which

$$\left.\begin{aligned} R &= \bar{S} \\ \text{and} \\ \cos\theta &= \frac{S_{ij}S^0_{ij}}{\bar{S}\bar{S}^0} \end{aligned}\right\}. \tag{57}$$

As the result of a prescribed increment in stress or strain, an algorithm will yield a final state S^F_{ij}, whereas the exact solution will, in general, be some other state S^E_{ij}. The corresponding coordinates of these two stress

points are (R_F, θ_F), and (R_E, θ_E), respectively. Then the error associated with the final state is completely def · · ›y an angle,

$$\bar{\theta} = \theta_F - \theta_E, \tag{58}$$

and the percentage difference in yield-surface radii,

$$\eta = 100 \frac{R_F - R_E}{R_E}. \tag{59}$$

For this study, the exact solution was defined to be the solution obtained with the use of N_e subincrements, where

$$N_e = 200(r + t). \tag{60}$$

The factor 200 was considered large enough, since values for $\bar{\epsilon}^p$ differed by less than 0.5% from corresponding values obtained with a factor of 100 for all choices of r and t. Typical engineering values of $E = 20.7 \times 10^9$ Pa, $H_0 = E/100$, and $\nu = 1/3$ were used for all cases.

Figures 2-4 show contour plots of errors obtained by the two algorithms when the final state was reached using a single step. For the elastic-perfectly plastic case, E_p is zero, and the yield-surface radius is fixed at the value R_0. Thus the error is defined in terms of a single parameter, $\bar{\epsilon}$, for which the results are shown in Fig. 2.

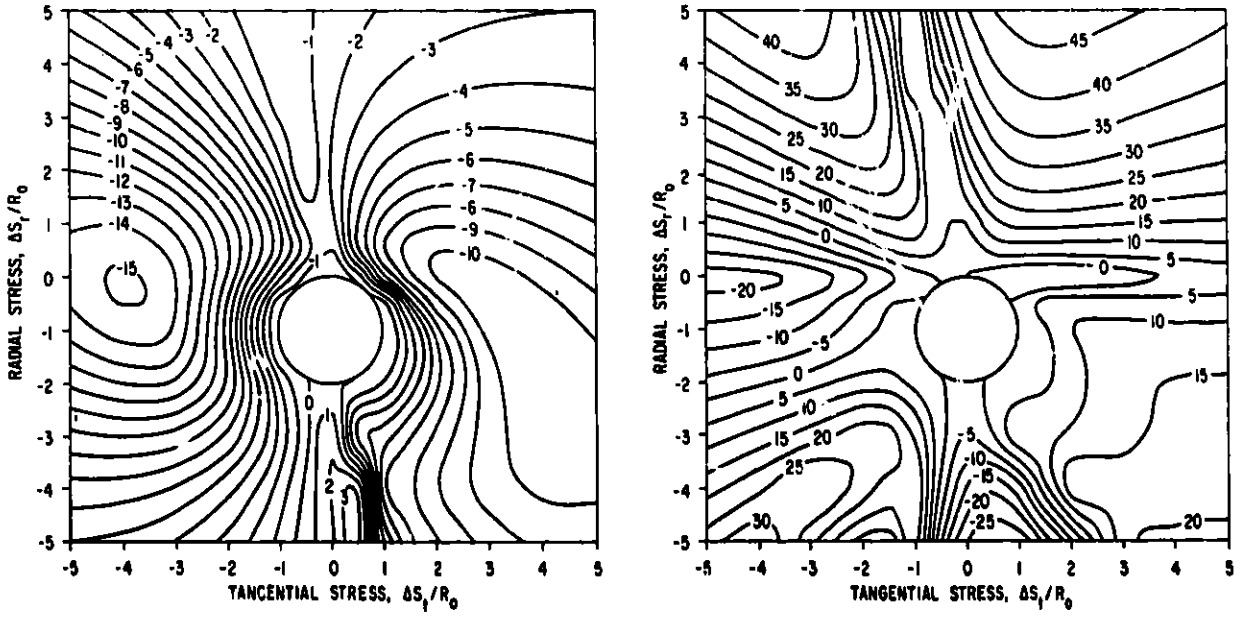

Fig. 2. Angular Error Contours for an Elastic-Perfectly Plastic Material ($E_p = 0$).
(a) Elastic Predictor, Radial Corrector; (b) Tangential Predictor, Radial Return.

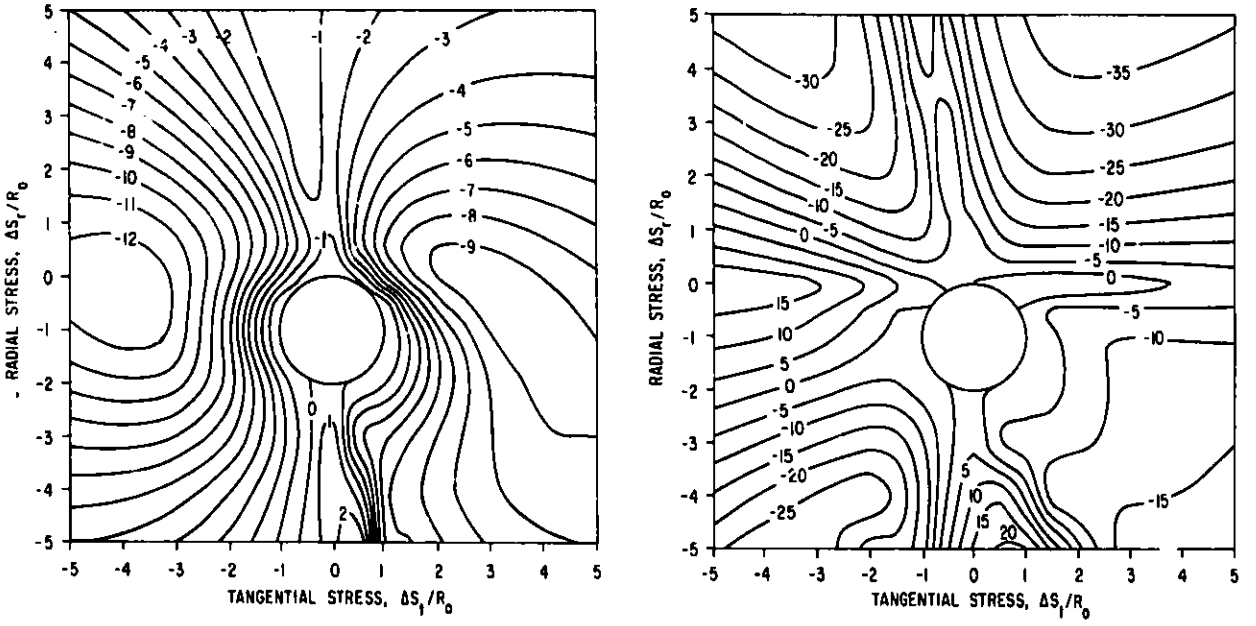

Fig. 3. Angular Error Contours for an Elastic–Plastic Material (E_p = E/10). (a) Elastic Predictor, Radial Corrector; (b) Tangent Predictor, Radial Return.

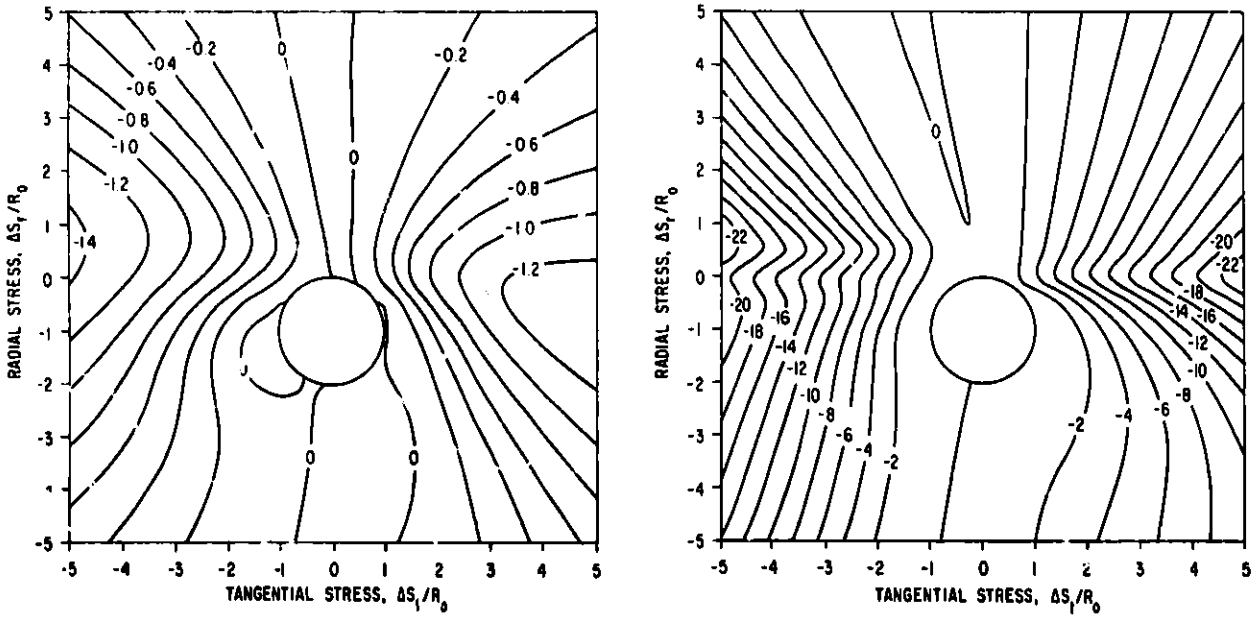

Fig. 4. Contour Plots of Percentage Error in Yield-surface Radii for an Elastic–Plastic Material (E_p = E/10). (a) Elastic Predictor, Radial Corrector; (b) Tangent Predictor, Radial Return.

An example involving a bilinear material with $E_p = E/10$ was also considered. Contours of the error angle are given in Fig. 3; contours of the percentage error in yield-surface radii are shown in Fig. 4.

Generally speaking, the error associated with the elastic-predictor/radial-corrector algorithm is much less for both the angular and radial measures than the error obtained with the tangent-predictor/radial-return method. This is in agreement with Krieg and Krieg's work[1] for an elastic-perfectly plastic material.

It should be emphasized that some of these steps are actually quite large and the assumption of a constant strain rate over the complete step can be very important. To illustrate the differences that can occur, selected load increments were covered in two steps over two paths. The first path consisted of the same strain-rate vector for each step; the second path consisted of a step with a purely tangential component in the principal-deviatoric-stress space followed by a purely radial step. The resulting errors in angle and radius for $E_p = E/10$ are summarized in Table I. The results, obtained with the elastic-predictor/radial-corrector algorithm, indicate that the use of a variable strain rate can introduce errors larger by one or two orders of magnitude if a constant strain rate is considered to be a valid assumption. Conversely, if the physical problem is one in which the strain-rate vector is changing, then the use of large constant-strain-rate steps can be the source of major errors.

TABLE I. Angular and Percentage Radial Errors for Two-step Stress Increments over Constant-strain-rate and Variable-strain-rate Paths (Elastic Predictor, Radial Corrector)

Components of Stress Increment (t, r)	Angular Error, $\bar{\theta}$		Error in Radius, $\bar{r}$	
	Constant Strain Rate	Two Strain Rates	Constant Strain Rate	Two Strain Rates
(4, 4)	-1.65	-20.78	-0.33	3.26
(-4, 4)	-3.06	-28.63	-0.44	6.68
(-4, -4)	-3.35	8.05	-0.37	19 03
(4, -4)	-5.20	30.72	-0.40	16.43

To evaluate the effect of subincrementation, Eq. 54 with k = 8 was used for the elastic-predictor algorithm and k = 4 for the tangent-predictor algorithm. Figures 5-7 are error-contour plots for elastic-perfectly plastic and elastic-plastic materials. The maximum number of subincrements, required for the elastic-predictor/radial-corrector and tangent-predictor/radial-return methods were 24 and 27, respectively. Note that, for approximately the same maximum number of subincrements, the maximum angular error is now less for the tangent-predictor scheme. Thus the use of subincrements in this case provides a much greater relative improvement for the tangent-predictor/radial-return algorithm than for the other method. However, the elastic-predictor/radial-corrector algorithm consistently provides lower

values of error for the yield-surface radii. In general, the results of both algorithms with subincrementation are considered to be satisfactory for most engineering problems.

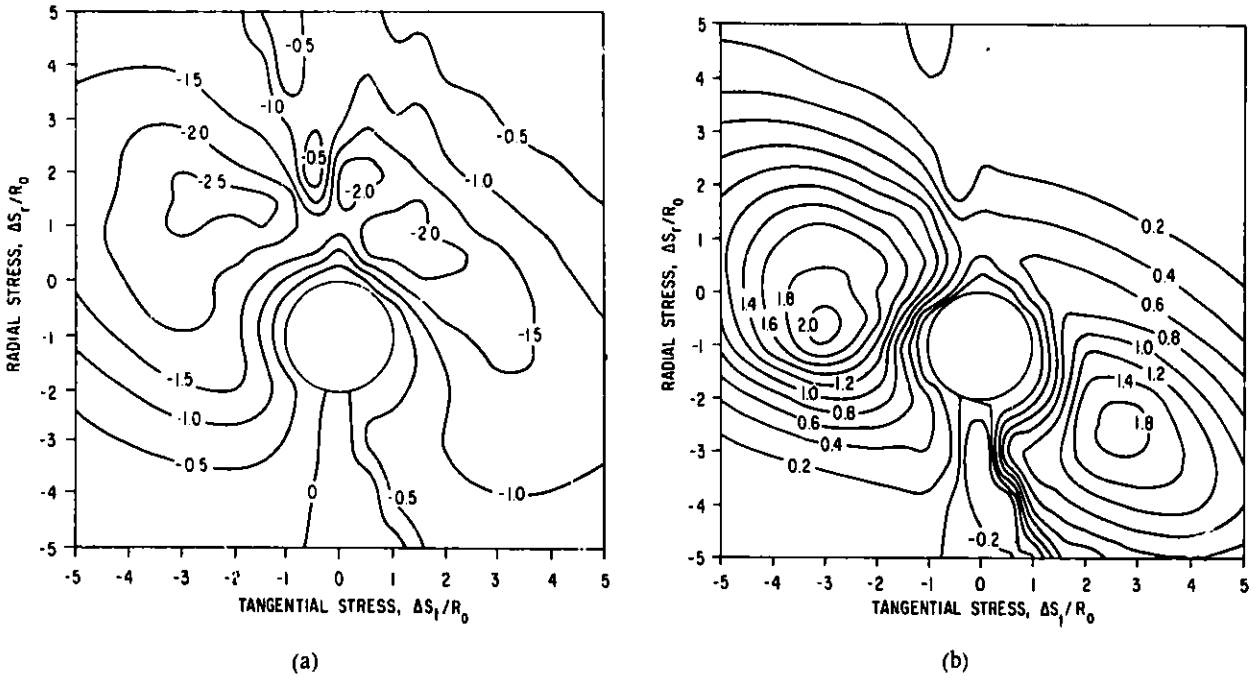

Fig. 5. Angular Error Contours for an Elastic–Perfectly Plastic Material with Subincrementation ($E_p = 0$). (a) Elastic Predictor, Radial Corrector; (b) Tangent Predictor, Radial Return.

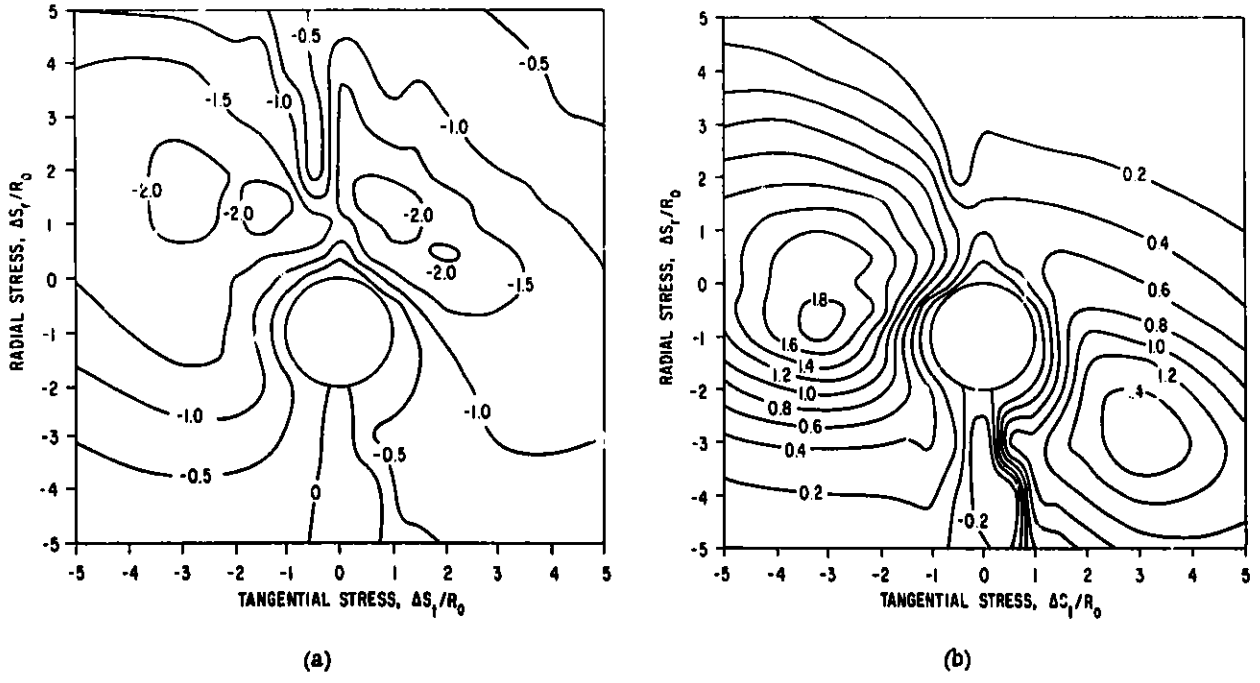

Fig. 6. Angular Error Contours for an Elastic–Plastic Material with Subincrementation ($E_p = E/10$). (a) Elastic Predictor, Radial Corrector; (b) Tangent Predictor, Radial Return.

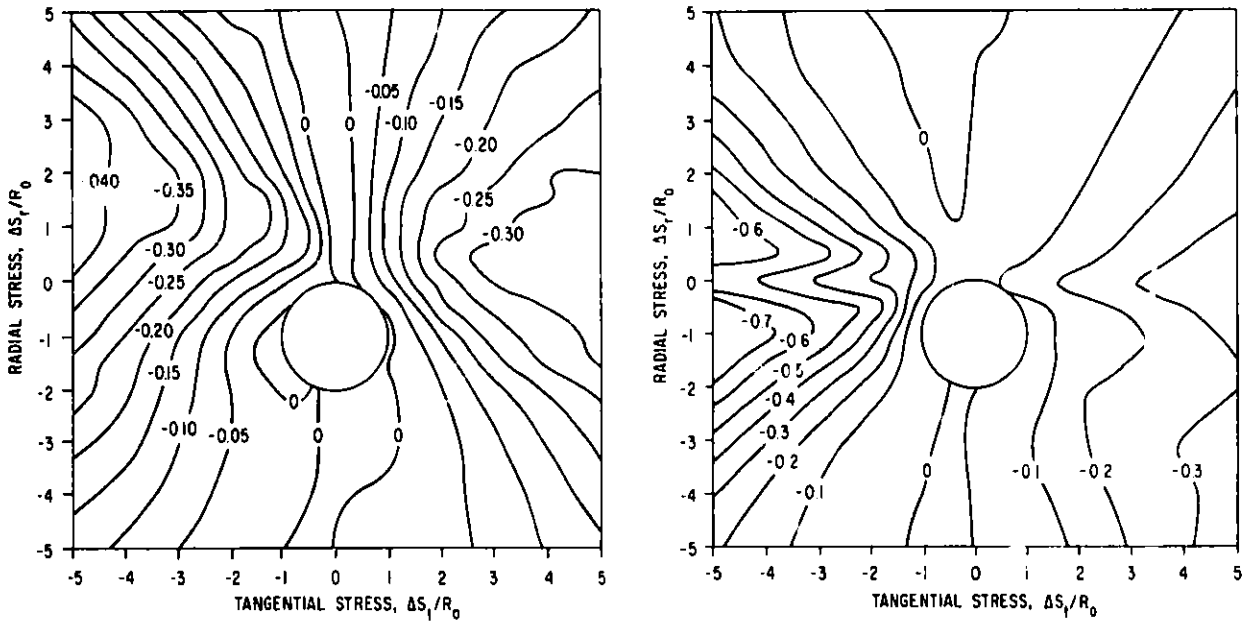

Fig. 7. Contour Plots of Percentage Error in Yield-surface Radii for an Elastic-Plastic Material with Subincrementation ($E_p = E/10$). (a) Elastic Predictor, Radial Corrector; (b) Tangent Predictor, Radial Return.

Since the symmetry in the principal-deviatoric-stress-rate space is destroyed with the plane-stress condition, different error contours are obtained if an alternative initial point S^0_{ij} is used. However, sample calculations indicate that, for any such point and for the given range of stress increments, the maximum values for error are approximately the same and of the same sign. Thus, the results cited above can be said to hold for an arbitrary starting point on the yield surface.

The results of Figs. 2-7 suggest that a combined algorithm might provide answers superior to either algorithm. An obvious possibility is the use of a tangent-predictor/radial-corrector scheme. Error contours for angles are only slightly different from those obtained previously (Fig. 3b) and hence are not shown. With regard to yield-surface radii there is a significant improvement over the tangent-predictor/radial-return scheme, as seen by comparing Figs. 4b and 8. However, now the error contours are all of a positive sign rather than the negative sign provided by each separate algorithm.

Error contours for the tangent-predictor/radial-corrector scheme with subincrementation (k = 4) were also obtained for a strain-hardening material. The maximum number of subincrements for this case was 27. Although the contour plots displayed different characteristics than those associated with the other two algorithms, the maximum values of error in angle and radius were of the same order of magnitude. Specifically, the maximum angular error was 2.2° and the radial error ranged from -0.6 to 2.0%.

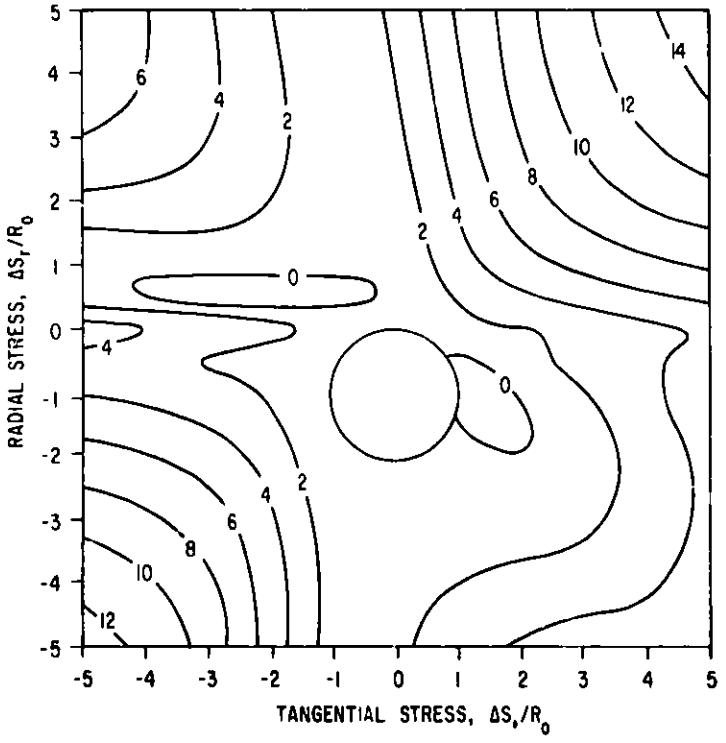

Fig. 8. Contour Plots of Percentage Error in Yield-surface Radii for an Elastic-Plastic Material with a Tangent-predictor/ Radial-corrector Algorithm

VII. CONCLUDING REMARKS

An error analysis for prescribed strain or stress steps has been performed for an elastic-predictor/radial-corrector, a tangent-stiffness/radial-return, and a combined tangent-stiffness/radial-corrector algorithm. A basic characteristic of this analysis is that results for a typical bilinear elastic-plastic material are not too different from those for an elastic-perfectly plastic material.

For a single-step approach, the elastic-predictor/radial-corrector algorithm produces much smaller errors than either of the other two algorithms over a wide range of prescribed stress or strain increments. However, with the use of approximately the same number of subincrements, the maximum error is of the same order of magnitude for each algorithm. The error associated with the subincrementation scheme is believed to be acceptable for a wide range of engineering problems.

As part of the detailed investigation of representative algorithms, a method was developed for conveniently describing and displaying errors, and the results were used as a guide for adopting an efficient subincrementation formula. This development was performed with the assumption of plane stress, because such a restriction introduces a degree of asymmetry and computational complexity that is not obvious from a strictly theoretical formulation. A similar investigation of the accuracy of other schemes for numerically evaluating elastic-plastic constitutive equations would be invaluable for rationally assessing the efficiency of each approach.

The algorithms studied have also been used for combined kinematic-isotropic hardening and for thermoplasticity. Although corresponding error analyses have not been performed under these conditions, it is believed that essentially the same characteristics would be displayed and that the subincrementation formula would be appropriate for these cases as well.

REFERENCES

1. R. D. Krieg and D. B. Krieg, *Accuracies of Numerical Solution Methods for the Elastic-Perfectly Plastic Model*, J. Pressure Vessel Technol., Trans. ASME *99*, J(4), 510-515 (1977).

2. S. W. Key, *HONDO--A Finite Element Computer Program for the Large Deformation Dynamic Response of Axisymmetric Solids*, Sandia Laboratories, SLA-74-0039 (Apr 1974).

3. A. Mendelson, *Plasticity: Theory and Application*, MacMillan Co., New York (1978).

4. P. V. Marcal, *A Stiffness Method for Elastic-Plastic Problems*, Int. J. Mech. Sci. *7*, 229-238 (1965).

5. P. V. Marcal, "Finite Element Analysis with Material Nonlinearities - Theory and Practice," in *Recent Advances in Matrix Methods of Structural Analysis and Design,* University of Alabama Press, 257-282 (1971).

6. Y. Yamada, N. Yoshimura, and T. Sakurai, *Plastic Stress-Strain Matrix and its Application for the Solution of Elastic-Plastic Problems by the Finite Element Method,* Int. J. Mech. Sci. *10,* 343-354 (1968).

7. D. Bushnell, *A Strategy for the Solution of Problems Involving Large Deflections, Plasticity and Creep,* Int. J. Numer. Methods Eng. *11,* 683-708 (1977).